Plant Biotechnology Journal

Plant Biotechnology Journal (2014), pp. 1–10 doi: 10.1111/pbi.12251

Monomeric IgA can be produced *in planta* as efficient as IgG, yet receives different *N*-glycans

Lotte B. Westerhof[1,*], Ruud H. P. Wilbers[1], Debbie R. van Raaij[1], Dieu-Linh Nguyen[2], Aska Goverse[1], Maurice G. L. Henquet[3], Cornelis H. Hokke[2], Dirk Bosch[3], Jaap Bakker[1] and Arjen Schots[1]

[1]*Plant Sciences Department, Laboratory of Nematology, Wageningen University and Research Centre, Wageningen, The Netherlands*

[2]*Department of Parasitology, Centre of Infectious Diseases, Leiden University Medical Center, Leiden, The Netherlands*

[3]*Plant Research International, Wageningen University and Research Centre, Wageningen, The Netherlands*

Received 28 May 2014;
revised 23 July 2014;
accepted 4 August 2014.
**Correspondence* (Tel +31317 485261;
fax +31317 484254;
email Lotte.Westerhof@wur.nl)
Accession numbers: The constant domains of human immunoglobulin alpha-1 (ACC82528.1), gamma-1 (AJ294730.1) and kappa (AGH70219.1) *Arabidopsis thaliana* chitinase gene (AAM10081.1).

Keywords: IgA, plant, *N*-glycosylation, Infliximab, Adalimumab, Ustekinumab.

Summary

The unique features of IgA, such as the ability to recruit neutrophils and suppress the inflammatory responses mediated by IgG and IgE, make it a promising antibody isotype for several therapeutic applications. However, in contrast to IgG, reports on plant production of IgA are scarce. We produced IgA1κ and IgG1κ versions of three therapeutic antibodies directed against pro-inflammatory cytokines in *Nicotiana benthamiana*: Infliximab and Adalimumab, directed against TNF-α, and Ustekinumab, directed against the interleukin-12p40 subunit. We evaluated antibody yield, quality and *N*-glycosylation. All six antibodies had comparable levels of expression between 3.5 and 9% of total soluble protein content and were shown to have neutralizing activity in a cell-based assay. However, IgA1κ-based Adalimumab and Ustekinumab were poorly secreted compared to their IgG counterparts. Infliximab was poorly secreted regardless of isotype backbone. This corresponded with the observation that both IgA1κ- and IgG1κ-based Infliximab were enriched in oligomannose-type *N*-glycan structures. For IgG1κ-based Ustekinumab and Adalimumab, the major *N*-glycan type was the typical plant complex *N*-glycan, biantennary with terminal *N*-acetylglucosamine, β1,2-xylose and core α1,3-fucose. In contrast, the major *N*-glycan on the IgA-based antibodies was xylosylated, but lacked core α1,3-fucose and one terminal *N*-acetylglucosamine. This type of *N*-glycan occurs usually in marginal percentages in plants and was never shown to be the main fraction of a plant-produced recombinant protein. Our data demonstrate that the antibody isotype may have a profound influence on the type of *N*-glycan an antibody receives.

Introduction

The use of monoclonal antibodies for the treatment of cancer, autoimmune diseases and inflammatory disorders is rapidly growing. Antibodies of the IgG isotype are most common, but other isotypes such as IgA may offer important advantages. IgA is best known as secretory IgA, a dimeric IgA complex enveloped by the secretory component, which helps protect mucosal surfaces against pathogens and control commensal bacteria. IgA is also the second most predominant isotype in the blood (Stoop *et al.*, 1969). In primates, serum IgA is monomeric, in contrast to other animals where serum IgA is dimeric. The immunotherapeutic potential of serum IgA has only been recognized recently, because the biology of serum IgA was poorly understood (Bakema and van Egmond, 2011; Snoeck *et al.*, 2006). Due to differences in IgA functioning between primates and other animals, a proper animal model was lacking. Most important in this regard is that rodents lack a homologue of the human Fc receptor for IgA (FcαRI or CD89) (Snoeck *et al.*, 2006). This already indicated that rodents lack an important effector function that is mediated by FcαRI in primates.

The creation of a transgenic mouse expressing human FcαRI helped reveal IgA's unique ability to recruit neutrophils, the largest population of white blood cells in the body (Van der Steen *et al.*, 2009). This capacity may be a valuable feature in cancer therapy, because IgA-induced tumour cell killing was shown to be mediated by neutrophils. IgG does not efficiently recruit neutrophils, but mediates cell lysis predominantly via the complement system and peripheral blood mononucleated cells (Huls *et al.*, 1999). In addition, serum IgA has immunosuppressive properties that may be of therapeutic interest. When free IgA associates with FcαRI on immune cells, inhibitory signals are triggered that block pro-inflammatory responses initiated by association of IgG and IgE with their Fc receptors. Thus, IgA may be used as an overall immune suppressor of inflammatory disorders (Bakema and van Egmond, 2011). The ability of IgA to suppress the immune response could be combined with the antigen-binding capacity. Many autoimmune and inflammatory disorders are nowadays treated by neutralization of pro-inflammatory cytokines using antibodies. Neutralization of the pro-inflammatory cytokine TNF-α is the most common therapy. Because TNF-α also occurs as a membrane-bound variant, use of an antibody directed

Please cite this article as: Westerhof, L.B., Wilbers, R.H.P., van Raaij, D.R., Nguyen, D.-L., Goverse, A., Henquet, M.G.L., Hokke, C.H., Bosch, D., Bakker, J. and Schots, A. (2014) Monomeric IgA can be produced *in planta* as efficient as IgG, yet receives different *N*-glycans. *Plant Biotechnol. J.*, doi: 10.1111/pbi.12251

against TNF-α not only results in neutralization of free TNF-α, but also results in neutrophil-mediated killing of immune cells harbouring TNF-α on their membrane (Shen *et al.*, 2005; Van den Brande *et al.*, 2003). Use of IgA may enhance killing of these immune cells through its previously mentioned unique ability to recruit neutrophils. As a consequence, this will result in better suppression of the immune response required for autoimmune and inflammatory disease treatment.

Most, if not all, therapeutic antibodies are made using mammalian cell lines. However, plants have been shown to be an excellent alternative production platform. Like animal cell lines, plants are capable of producing high levels of complex proteins, but are easier to manipulate and more economic in use (Hiatt and Pauly, 2006; Schillberg *et al.*, 2003). Next to that, plant-produced proteins often appear more homogeneously glycosylated compared to proteins produced by mammalian cell lines (Cox *et al.*, 2006). Engineering of the *N*-glycosylation machinery has been successful in plants, and research on humanizing *N*-glycosylation in plants has advanced over the last decade, allowing production of antibodies and other proteins with human *N*-glycan types (Bosch *et al.*, 2013; Castilho *et al.*, 2011; Strasser *et al.*, 2009). However, most of this work has been based on the plant expression of IgG antibodies, and few reports on the plant expression of IgA exist (De Muynck *et al.*, 2010). The few IgA antibodies that have been produced in plants were based on a variety of IgA backbones (murine, chicken and human), were expressed in different plant species (tobacco, maize, rice, tomato and *Arabidopsis*) and demonstrated a great variability in yield (Juarez *et al.*, 2012; Karnoup *et al.*, 2005; Ma *et al.*, 1994; Nakanishi *et al.*, 2013; Nicholson *et al.*, 2005; Wieland *et al.*, 2006).

To obtain insight in the effect of isotype on the yield, quality and *N*-glycosylation of antibodies when expressed in plants, we compared the expression of monomeric IgA and IgG in *Nicotiana benthamiana*. Thereto we expressed the therapeutic antibodies Infliximab, Adalimumab and Ustekinumab in their original form as IgG1κ antibodies as well as the IgA1κ variants of these three antibodies. Both Infliximab and Adalimumab are directed against TNF-α. Infliximab is a chimeric antibody with mouse variable regions on a human backbone (Ebert, 2009), and Adalimumab is a fully human antibody (Bain and Brazil, 2003). Ustekinumab is a human antibody directed against the interleukin-12 p40 subunit (IL-12p40) shared by the pro-inflammatory cytokines IL-12 and IL-23 (Gandhi *et al.*, 2010). All three antibodies are used to treat several inflammatory disorders such as rheumatoid arthritis, psoriasis and inflammatory bowel disease. Upon plant expression, we observed a similar high yield and quality of the IgA1κ-based antibodies compared to the original IgG1κ variants. The *N*-glycosylation pattern, however, was different. While IgG-based antibodies predominantly carried the typical plant complex *N*-glycan for secreted proteins, a biantennary *N*-glycan with terminal *N*-acetylglucosamine (GlcNAc) with β1,2-xylose and core α1,3-fucose ($GnGnXF^3$), IgA-based antibodies lacked core α1,3-fucose and one terminal GlcNAc (GnMX or MGnX).

Results

Antibody isotype and idiotype have little effect on yield

To establish the production potential of human IgA in plants, we investigated the expression of the variable regions of the three therapeutic antibodies Infliximab (I), Adalimumab (A) and Ustekinumab (U) on both a human IgA1κ and human IgG1κ backbone *in planta* (Figure 1a). Light chain (κ) and either the alpha (α)-1 or gamma (γ)-1 heavy chain were combined in one expression vector and transiently expressed in *N. benthamiana*. Yield was determined up to 15 days postinfiltration (dpi) with 3-day intervals. Figure 1b shows the average recombinant protein levels of three biological replicates. IgG yields peaked at dpi 6 with 82, 90 and 68 μg of antibody (Ab) per mg of total soluble protein (TSP) for IgG-I, IgG-A and IgG-U, respectively. IgA yields peaked on later time points at dpi 9 for IgA-I and IgA-U and dpi 12 for IgA-A. Although prolonged accumulation can be indicative of greater protein stability, the overall yield of the IgA's is lower, 35, 70 and 46 μg Ab/mg TSP for IgA-I, IgA-A and IgA-U, respectively. Thus, antibody yield most likely depends more on the expression system than idiotype or isotype.

Plants produce high-quality IgA antibodies

To investigate protein quality, the antibodies were analysed by Western blot. Figure 2 shows the visualization of the κ, γ and α chains when samples were run under reduced conditions. For all antibodies, the predominant band of the heavy chain migrated at the expected size (~49 and ~51 kDa for the γ and α chain, respectively). For α-A, α-U and the recombinant control, a doublet (two bands migrating very close to each other) was observed. As the constant region of α-1 has two *N*-glycosylation sites, these bands can represent α chains with none, one or two *N*-glycans. Surprisingly, α-I shows only the higher of the two bands observed for α-A, α-U and the recombinant control. This suggests that the α-I chain lacks either the unglycosylated or the one-time glycosylated variant of α-I. The κ-A and κ-U chains also had the expected size (~23.5 kDa), while κ-I had a slightly higher molecular weight. Because no *N*-glycosylation sites are present in the κ chains, this difference cannot be explained by differences

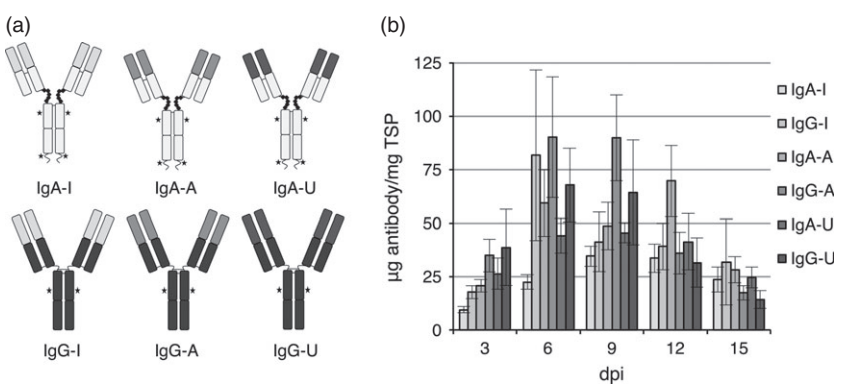

Figure 1 Plant production of IgA1κ and IgG1κ antibodies. (a) Cartoon representing the expressed antibodies. (b) Yield of Infliximab (I), Adalimumab (A) or Ustekinumab (U) on an IgA1κ or IgG1κ backbone when transiently expressed in *Nicotiana benthamiana* up to 15 days postinfiltration (dpi). Bars indicate average yield, and error bars indicate standard error (n = 3). *position of N-glycans.

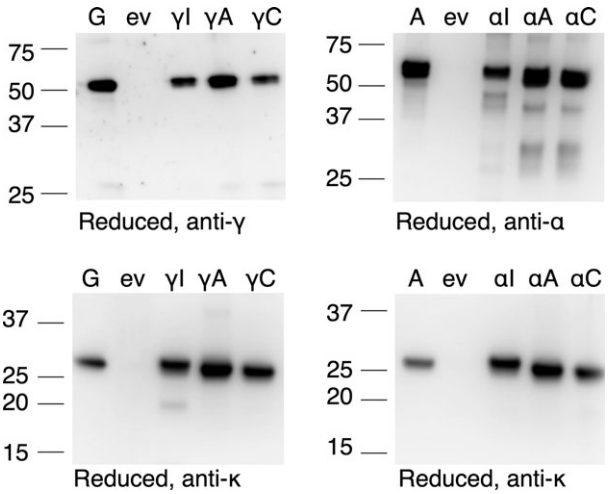

Figure 2 Evaluation of quality of plant-produced IgA1κ and IgG1κ antibodies. Western blots under reducing conditions of 50 ng Infliximab (I), Adalimumab (A) or Ustekinumab (U) on an IgA1κ or IgG1κ backbone in leaf extracts visualizing the kappa chain (κ), gamma chain (γ) or alpha chain (α), as indicated. Recombinant IgG (G) or IgA (A) and empty vector (ev) control were included.

in *N*-glycosylation. Comparison of plant-produced κ-I to the murine myeloma cell line produced κ-I showed equal electrophoretic mobility. This suggests that intrinsic properties of the variable domain lead to aberrant running behaviour and do not indicate an actual increase in molecular weight (data not shown).

For the α chains, several additional bands were observed that migrated faster than the expected size. These additional bands most likely represent proteolytic degradation products. A different pattern can be seen for α-I compared to α-A and α-U. It is possible that α-I is sensitive to other proteases than the other two chains or that IgA-I is exposed to different proteases, which would suggest a different intracellular location of this antibody. Alternatively, the bands of α-I represent different *N*-glycan variants of the same degradation products. For κ-I, it was striking to observe that an additional band migrating around 20 kDa was only seen when co-expressed with the γ heavy chain, but not α heavy chain. It most likely also represents a degradation product that may be the consequence of a different conformation of IgA-I and IgG-I, whereby κ-I is more susceptible to proteases when it is associated with the γ-I chain than the α-I chain. Alternatively, IgG-I subcellular targeting may be different to IgA-I and therefore may encounter different proteases. Whatever the cause of the differences in degradation products between the antibody chains, the majority of each antibody chain appears to be intact.

Efficiency of antibody secretion from plant cells depends on isotype and idiotype

As antibodies are secretory proteins, we developed a method to compare secretion efficiency of proteins as an indicator of aberrant subcellular targeting. The amount of secreted antibody was determined by 'washing out' the apoplast fluid from the transformed leaf followed by isolation of intracellular proteins and determination of antibody concentration in both fractions. Figure 3a shows the secretion efficiency of all six antibodies as the means of three biological replicates. Independent of idiotype, IgG secretion was at least three times more efficient than IgA secretion. Poor secretion of a murine IgA/IgG chimera from plant cells was demonstrated before (Frigerio *et al.*, 2000). This murine IgA/G chimera was targeted to the vacuole due to a cryptic sorting signal in the tailpiece of murine IgA (Hadlington *et al.*, 2003). Human IgA has a similar tailpiece, although the sequence differs from mouse IgA. To reveal whether or not poor secretion of human IgA is also caused by its tailpiece, a variant of IgA-U without tailpiece (IgA-UΔT) was expressed, and its secretion efficiency was determined (Figure 3b). While the average yield of IgA-UΔT was similar, the secretion efficiency was enhanced more than twofold. Like the murine tailpiece, the human tailpiece may be responsible for the poor secretion as a consequence of vacuolar targeting.

To evaluate whether the degradation products described in the previous section were caused by protease activity inside the cell or in the apoplast, both intracellular and apoplast fractions were evaluated by Western blot analysis (Figure 3c). As all apoplast fractions were enriched with the degradation products, we assume that most, if not all, proteolytic degradation takes place in the apoplast. This explains why the degradation product of κ-I that was only detected upon co-expression with the γ chain, but not the α-chain, as 10% of IgG-I compared to only 1.8% of IgA-I was secreted.

The secretion efficiency between idiotypes also differed. IgG-I secretion was two times less efficient compared to IgG-A and

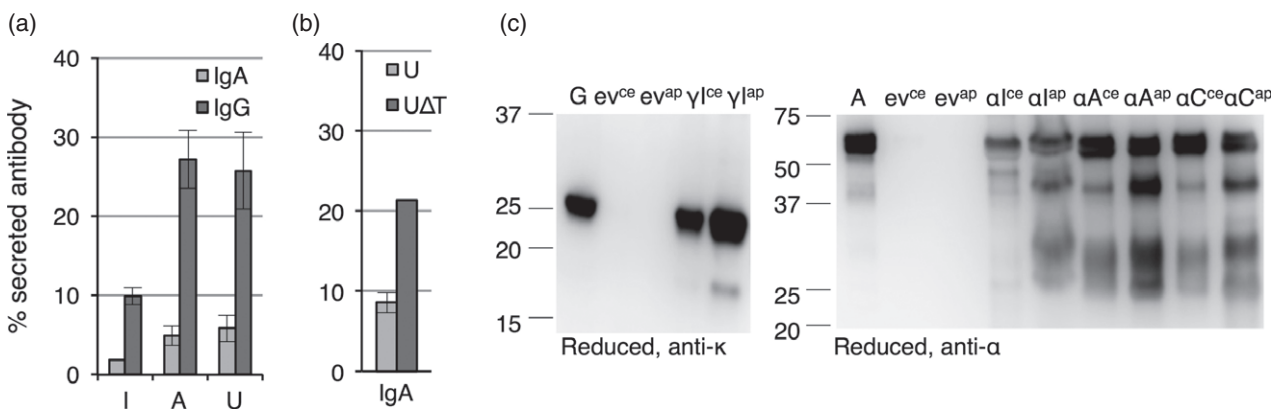

Figure 3 Secretion and proteolytic degradation of plant-produced IgA1κ and IgG1κ antibodies. (a,b) Percentage of secretion of IgG1κ and IgA1κ by determining the amount of antibody in apoplast fluids (ap) versus crude extracts (ce) (n = 3, error bars indicate standard error). (c) Western blot analysis under reducing conditions of 50 ng Infliximab (I), Adalimumab (A) and Ustekinumab (U) with and without tailpiece (ΔT) on an IgA1κ or IgG1κ backbone visualizing the kappa chain (κ) or alpha heavy chain (α), as indicated. Recombinant IgG (G) or IgA (A) and empty vector (ev) control were included.

IgG-U secretion. The same result was obtained comparing the IgA antibodies. Apparently, both isotype and idiotype are important for secretion efficiency.

Differential *N*-glycosylation of IgA compared to IgG

Because differences in subcellular localization can influence *N*-glycosylation, we evaluated *N*-glycan maturity of all antibodies. Thereto the antibodies were treated with the enzymes peptide:
N-glycosidase F (PNGase F) or endoglycosidase H (Endo H) followed by Western blot analysis. PNGase F only cleaves *N*-glycans which lacks the plant-specific α1,3-fucose, while Endo H only cleaves oligomannose-type *N*-glycans. Treatment of the IgG antibodies with either enzyme did not reduce heavy chain size, except the recombinant control (G), which became smaller upon PNGase F treatment (Figure 4, top panel). This indicates that the plant-produced IgG antibodies do not carry oligomannose-type *N*-glycans and confirms the presence of the plant-specific α1,3-fucose. In contrast, when the IgA-A and IgA-U antibodies were treated with PNGase F, a major fraction of the α heavy chains was reduced in size (Figure 4, second panel). EndoH did not affect IgA-A and IgA-U. This suggests that a major fraction of IgA-A and IgA-U carry complex-type *N*-glycans that are devoid of core α1,3-fucose. Treatment of IgA-I with Endo H or PNGaseF caused a reduction in size of the α-I chain, suggesting that IgA-I carries oligomannose-type *N*-glycans.

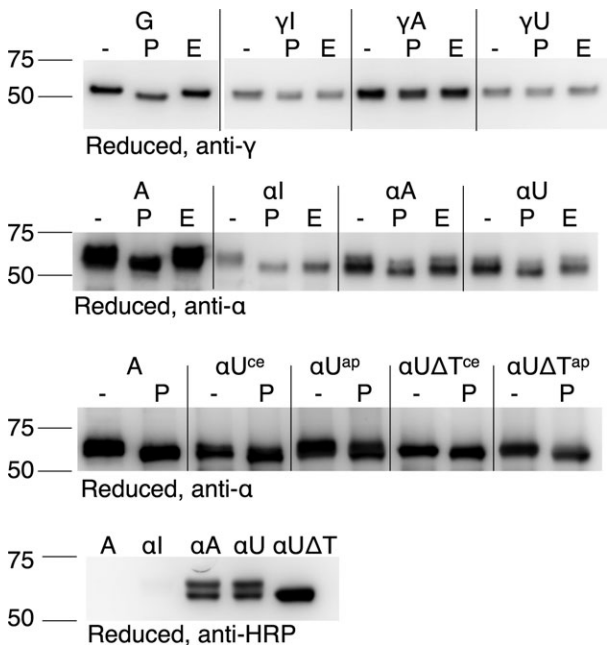

Figure 4 Evaluation of *N*-glycan maturity of plant-produced IgA1κ and IgG1κ antibodies. Western blots under reducing conditions of 50 ng purified Infliximab (I), Adalimumab (A) or Ustekinumab (U) on an IgG1κ or IgA1κ backbone with or without tailpiece (ΔT) visualizing the gamma heavy chain (γ), the alpha heavy chain (α) or β1,2xylose/α1,3-fucose (HRP), as indicated. Ustekinumab (U/UΔT) was isolated from apoplast (ap) or crude extract (ce) and was analysed separately by visualizing the alpha heavy chain (α). Recombinant IgG (G) or IgA (A) and an empty vector (ev) were included. Samples were treated with Endo H (H) or PNGase F (P) to screen for the presence of oligomannose-type *N*-glycans or α1,3-fucose, respectively.

To determine whether the atypical *N*-glycosylation of IgA-A and IgA-U is the result of poor secretion of IgA, both IgA-U and IgA-UΔT from the apoplast or crude leaf extract were evaluated by treatment with PNGase F (Figure 4, third panel). Treatment with PNGase F reduced the major fraction of the α heavy chains in size of both intracellular and secreted IgA-U and IgA-UΔT. This suggests that the absence of a core α1,3-fucose on *N*-glycans of IgA does not depend on its subcellular targeting. Furthermore, the fact that IgA-UΔT shows only one band that is sensitive to PNGase F suggests that this band represents a glycosylated α chain. Because one of the *N*-glycan sites of human IgA resides in the tailpiece, IgA-UΔT cannot carry more than one *N*-glycan. The absence of a second band for nonglycosylated IgA-UΔT therefore indicates that the *N*-glycan site in constant domain 2 must always receive an *N*-glycan. The doublet in IgA-A and IgA-U must therefore be the result of partial *N*-glycosylation of the tailpiece.

To assess the presence of β1,2-xylose on the IgA antibodies, a Western blot was performed using a polyclonal rabbit antihorseradish peroxidase antibody specific for plant α1,3-fucose and β1,2-xylose (Figure 4, bottom panel). For both IgA-A and IgA-U, two bands appeared confirming the presence of β1,2-xylose on both *N*-glycan variants. For IgA-UΔT, only one band appeared due to the absence of the *N*-glycosylation site present in the tailpiece.

To obtain a more detailed picture, we analysed the composition of the *N*-glycans on the plant-produced antibodies using matrix-assisted laser desorption/ionization time-of-flight mass spectrometry (MALDI-TOF-MS) (Table 1). For IgG, tryptic glycopeptides were prepared prior to MALDI-TOF-MS analysis. As predicted, the major *N*-glycan type present on IgG glycopeptides was identified as the typical plant complex *N*-glycan for secreted proteins, a biantennary *N*-glycan with terminal GlcNAc with β1,2-xylose and core α1,3-fucose ($GnGnXF^3$) (Figure S1). Surprisingly, IgG-I carried a small fraction of oligomannose-type *N*-glycans, which may be indicative of ER retention. This is in line with the

Table 1 Major *N*-glycan types carried by the plant-produced IgA1κ or IgG1κ variants of Infliximab (I), Adalimumab (A) and Ustekinumab (U) as determined using MALDI-TOF-MS (Figures S1 and S2)

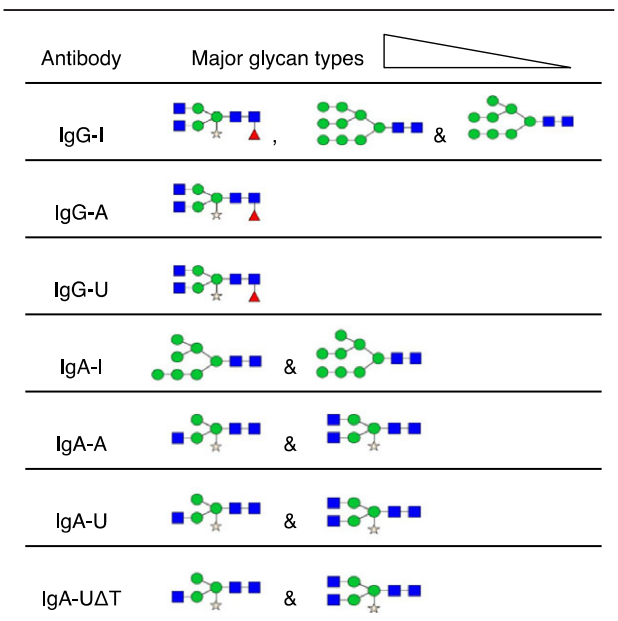

fact that IgG-I was less efficiently secreted compared to IgG-A and IgG-U (Figure 3).

Analysis of IgA *N*-glycans based on tryptic glycopeptides was not successful. Tryptic digestion of IgA results in relatively large glycopeptides compared to IgG and might therefore not be suitable for this approach. Alternatively, IgA was digested with either trypsin, pepsin or thermolysin, followed by PNGase A release of *N*-glycans. Unfortunately, this approach did also not result in clear *N*-glycan profiles. Because we already confirmed that the majority of the *N*-glycans on plant-produced IgA do not carry α1,3-fucose, we used PNGase F to release *N*-glycans from IgA, and this did result in clear *N*-glycan profiles (Figure S2). The *N*-glycan profiles for IgA revealed that IgA-I carries mainly oligomannose-type *N*-glycans. The predominant *N*-glycan type found on IgA-A, IgA-U and IgA-UΔT was similar to IgG, but lacked one terminal GlcNAc. Although we cannot exclude that *N*-glycans on plant-produced IgA may occasionally carry a core α1,3-fucose, we can assume that the predominant *N*-glycan on plant-produced IgA-A, IgA-U and IgA-UΔT is GnMX or MGnX. In conclusion, it seems that the *N*-glycan type that an antibody receives upon expression *in planta* is mainly determined by the antibody isotype.

Antigen-binding capacity

To determine the antigen-binding capacity of the plant-produced antibodies, cell-based assays were performed. For Infliximab and Adalimumab, which are directed against TNF-α, we assessed the capacity of these antibodies to abrogate TNF-α induced apoptosis of L929 cells. For Ustekinumab, which is directed against the p40 subunit of IL-12 and IL-23, its capacity to block IL-23-induced production of IL-17 by murine splenocytes was assessed.

Cell viability of L929 cells increased in a dose-dependent manner upon increasing concentration of plant-produced IgG-I, IgA-I, IgG-A and IgA-A, but not plant-produced IgG-U and IgA-U, which were used as negative controls (Figure 5a). No significant difference was observed between the murine myeloma cell (SP2/0) produced Infliximab and plant-produced IgG-I, IgA-I, IgG-A and IgA-A. It is surprising that IgG-I and IgA-I perform equally well when compared to the control in this assay as both antibodies were enriched in oligomannose-type *N*-glycan structures that may indicate improper protein folding.

IL-17 production reduced in a dose-dependent manner upon increasing concentration of both plant-produced IgG-U and IgA-U, but not plant-produced IgG-I and IgA-I, which were used as negative controls (Figure 5b). No significant difference was observed between the murine myeloma cell (SP2/0) produced Ustekinumab and the plant-produced variants.

Thus, regardless of the antibody isotype, plants produce functional Infliximab, Adalimumab and Ustekinumab.

Discussion

Currently, most therapeutic antibodies are of the IgG isotype. Yet, IgA was suggested as a promising alternative isotype that may increase the therapeutic opportunities of several antibody-based therapies (Bakema and van Egmond, 2011). Therefore, we evaluated the plant production of IgA. We expressed IgA1κ variants of the three commercially available therapeutic antibodies, Infliximab, Adalimumab and Ustekinumab in *N. benthamiana*. The production of the IgA1κ variants was compared to the production of their original form as IgG1κ antibodies. Expression of all six antibodies was successful with high yields ranging from 3.5% to 9% of total soluble protein, whereby IgG performed slightly better for all three antibodies. Although the majority of the antibodies remained intact, IgA was found to be somewhat more sensitive to proteolytic enzymes than IgG. Many reports on the plant expression of IgG exist, but these are often based on the expression of a single antibody. Comparing the results of these reports reveals a large heterogeneity in antibody quantity and quality, whereby antibody yield varies several orders of magnitude (De Muynck *et al.*, 2010). However, our data reveal only slight discrepancies in antibody quantity and quality between isotypes and idiotypes, indicating that the previously reported heterogeneity may largely be attributed to, for example, differences in transformation method, subcellular targeting, and use of plant tissue and species.

In line with previous reports on *N*-glycosylation of plant-expressed IgG's, all our IgG-based antibodies predominantly carried the typical complex plant *N*-glycan for secreted proteins,

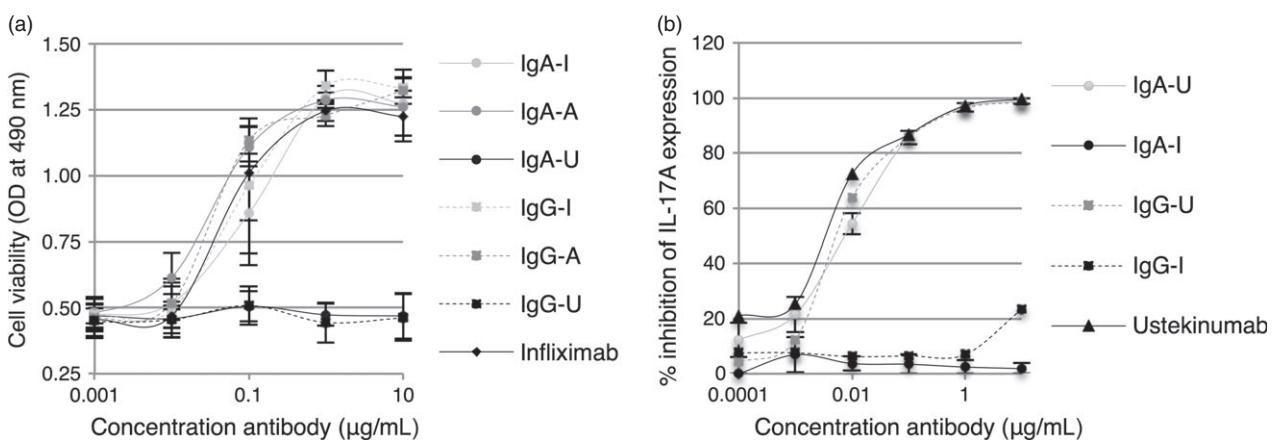

Figure 5 Biological activity of plant-produced IgA1κ and IgG1κ antibodies. (a) Cell viability of L929 cells when exposed to TNFα in combination with different concentrations of plant-produced Infliximab (I), Adalimumab (A) and Ustekinumab (U) on an IgG1κ or IgA1κ backbone. Mammalian cell-produced Infliximab (IgG) and a commercially available anti-TNFα IgA were included. (b) IL-17 production by murine splenocytes exposed to IL-23 in combination with different concentrations of plant-produced Infliximab (I) and Ustekinumab (U) on an IgG1κ or IgA1κ backbone. Mammalian cell-produced Ustekinumab (IgG) was included. Bars indicate averages, and error bars indicate standard error (n = 3).

biantennary with terminal GlcNAc and β1,2-xylose and core α1,3-fucose ($GnGnXF^3$). However, our IgA-based Adalimumab and Ustekinumab predominantly carried a similar *N*-glycan type as IgG, but lacked core α1,3-fucose and one terminal GlcNAc (GnMX or MGnX). Oligomannose-type *N*-glycans were found on both the IgG and IgA variants of our plant-produced Infliximab. On IgG, Infliximab oligomannose was found to a minor extent; however, on IgA Infliximab, this was the predominant *N*-glycan type.

Differences in *N*-glycosylation may be caused by differences in subcellular targeting. Infliximab was less efficiently secreted into the apoplast compared to Adalimumab and Ustekinumab, regardless of isotype backbone. This coincided with the presence of oligomannose-type *N*-glycans. Oligomannose-type *N*-glycans on heterologously expressed proteins are often indicative of retention in the endoplasmic reticulum (ER) and are associated with protein misfolding. Because only our IgG- and IgA-based Infliximab showed enrichment of oligomannose-type *N*-glycans, improper processing of Infliximab chains *in planta* seems a logical explanation for the presence of these *N*-glycan types. As protein misfolding is coupled with protein degradation, the yield of a misfolded protein is expected to be low. However, we did not find significantly lower yields for both isotypes of Infliximab compared to the yields of Adalimumab and Ustekinumab. Also, both IgG- and IgA-based Infliximab showed the same capacity to neutralize TNF-α when compared to murine myeloma cell (SP2/0) produced Infliximab. Still, oligomannose enrichment was only demonstrated for IgG and IgA infliximab and must therefore depend on idiotype. In conclusion, as folding of Infliximab leads to functional antibodies, the reason for oligomannose enrichment remains to be elucidated.

Evaluation of the secretion efficiency of all antibodies revealed that the IgA variants were secreted less efficiently into the apoplast when compared to IgG. A previous study demonstrated that plant-based expression of a chimeric murine IgG/A antibody resulted in targeting of this antibody to the lytic vacuole. A cryptic targeting signal in the tailpiece of the antibody was responsible for vacuolar targeting (Frigerio *et al.*, 2000; Hadlington *et al.*, 2003). Upon arrival in the vacuole, the murine G/A chimera underwent proteolytic degradation. We also found degradation products of our IgA-based antibodies, while no degradation was observed for the IgG-based variants. However, IgA isolated from the apoplast showed more prominent degradation than intracellular IgA. Thus, in contrast to the murine G/A chimeric antibody, degradation of human IgA likely resulted from proteolysis in the apoplast. In the C-terminus of the vacuolar proteins, tobacco β-glucanase and potato PT20, the dipeptides VS and SV are present (Koide *et al.*, 1999; Vitale and Raikhel, 1999). The murine tailpiece contains the sequence 'VSVSV', a repetition of VS and SV, and was therefore suggested to be the cryptic vacuolar targeting. The human tailpiece contains the sequence 'VSV' which may fulfil the same role. However, the human tailpiece also contains the dipeptides 'AE', which is a conserved motif in vacuolar targeting signals of several *Graminea* lectins (Bednarek *et al.*, 1990), and 'VD', found in the vacuolar targeting signal of tobacco chitinase A (Neuhaus *et al.*, 1991). These proteins are supposedly sorted to the protein storage vacuole (Neuhaus and Rogers, 1998), which may also be the destination of human IgA. Targeting to the protein storage vacuole instead of the lytic vacuole would explain the absence of proteolytic products of intracellular IgA as well as the fact that yield reduction in comparison to IgG was minor.

Golgi dependent and independent vacuolar targeting pathways have been identified (Park *et al.*, 2004), and the route taken seems to depend on protein intrinsic properties. Because the attachment of β1,2-xylose occurs in the *medial* Golgi (Fitchettelaine *et al.*, 1994; Rayon *et al.*, 1998), our IgA-based antibodies must travel to the Golgi as the *N*-glycans on our IgA-based Adalimumab and Ustekinumab carried this sugar residue. After attachment of β1,2-xylose, the core α1,3-fucose sugar residue is added in the *trans* Golgi (Fitchettelaine *et al.*, 1994; Rayon *et al.*, 1998). The core α1,3-fucose sugar residue is absent from the majority of the *N*-glycans of our IgA-based Adalimumab and Ustekinumab. Thus, the lack of core α1,3-fucose could be explained by vacuolar targeting if IgA is transported to the vacuole from the *medial* Golgi. However, the core α1,3-fucose was also absent from the *N*-glycans of secreted IgA-based Ustekinumab, which must have travelled through the *trans* Golgi to reach the apoplast.

Another, more plausible, reason for the lack of core fucosylation may be found in the protein intrinsic properties. Petrescu *et al.* (2004) analysed the protein environment of *N*-glycosylation sites and demonstrated that many *N*-glycan sites are poorly accessible (Petrescu *et al.*, 2004). As a result, *N*-glycans lacking one or more sugar residues are found, because the core of a *N*-glycan cannot always be reached by core altering glycosyltransferases. On human serum, IgA less than half of the *N*-glycans carry the typical mammalian core α1,6-fucose (Field *et al.*, 1994; Mattu *et al.*, 1998), whereas 80–98% of the *N*-glycans on human serum IgG antibodies are core fucosylated (Pucic *et al.*, 2011). IgG and IgA are both *N*-glycosylated in constant domain 2 (Cγ2 and Cα2, respectively), and structurally, these domains are similar. The major differences between these domains are the positions of interdomain disulphide bridges and the *N*-glycans (Herr *et al.*, 2003). The *N*-glycans of Cγ2 of IgG stabilize the interaction between the γ heavy chains, whereas in IgA, this is performed by a disulphide bridge. Compared to IgG, the *N*-glycans of the Cα2 domain of IgA are overall more exposed and therefore more accessible for processing (Yoo *et al.*, 2010). This may explain why these *N*-glycans have increased sialylation and galactosylation compared to *N*-glycans of IgG (Mattu *et al.*, 1998). However, this does not rule out the possibility that the core of these *N*-glycans have lower accessibility for core altering enzymes compared to IgG.

Alternatively, specific amino acids surrounding the *N*-glycosylation site may interfere with efficient core fucosylation. While evaluating the direct surroundings of the *N*-glycosylation sites of human IgG1 and IgA1 (position −3 to +4 from the asparagine in the N-X-S/T site), the only observed consistent difference was the presence of the hydrophobic amino acids leucine or valine on position X of the *N*-glycosylation sites of IgA1, whereas IgG1 contains a hydrophilic serine. We found this striking as chicken ovalbumin also contains a leucine on position X of its *N*-glycosylation signal, and when we expressed ovalbumin in plants, the core α1,3-fucose was absent from this *N*-glycan as well (L. B. Westerhof, R. H. P. Wilbers, D. R. van Raaij, E. Capuder, D.-L. Nguyen, M. G. L. Henquet, C. H. Hokke, D. Bosch, J. Bakker & A. Schots, unpublished data). Also plant-produced ovalbumin was insensitive towards PNGase A digestion. We therefore hypothesize that protein intrinsic properties that might interfere with core α1,3-fucosylation could also interfere with PNGase A release of *N*-glycans for MALDI-TOF-MS analysis. How amino acids surrounding the *N*-glycan site can influence core fucosylation or *in vitro* *N*-glycan release may become apparent when

more *N*-glycan profiles from plant-produced proteins become available in the future.

Next to the core α1,3-fucose, a terminal GlcNAc was lacking on IgA-based Adalimumab and Ustekinumab. Although GnM or MGn-type *N*-glycans occur in marginal percentages in plants, most proteins carry either MM (paucimannosidic) or GnGn-type *N*-glycans. MM-type *N*-glycans are the result of the activity of enzymes that remove terminal GlcNAc's. Three enzymes (HEXO1–3) capable of removing terminal GlcNAc residues were identified in *Arabidopsis* and shown to localize to the vacuole (HEXO1) and plasma membrane (HEXO2/3) (Liebminger *et al.*, 2011; Strasser *et al.*, 2007). Therefore, *N*-glycans on secreted as well as vacuolar proteins can be modified in this manner. All three enzymes were demonstrated to remove the terminal GlcNAc residues from both α1,3- and α1,6-branched mannoses without strict preference. Thus, subcellular targeting cannot explain why only one terminal GlcNAc would be removed and not the other. The underlying mechanism controlling GlcNAc removal is unclear, but seems to depend on protein intrinsic properties. It is possible that the GlcNAc's are inefficiently removed from the *N*-glycans of IgA resulting in a mix of GnMX- and MGnX-type glycans. Alternatively, it is also possible that one of the terminal GlcNAc's is not added. If this is the case, the α1,6-branched mannose must not have received its GlcNAc, as β1,2-xylose was present, and the terminal GlcNAc on the α1,3-branched mannose is required for β1,2-xylosyltransferase activity (Kajiura *et al.*, 2012). *N*-acetylglucosaminyltransferase II (GnT-II) is the enzyme responsible for the addition of a GlcNAc to the α1,6-branched mannose. Thus, for unknown reasons, it is possible that GnT-II does not act on *N*-glycans of IgA. This would, however, be a matter of efficiency, as we did find a proportion of *N*-glycans with terminal GlcNAc's on both arms on our IgA-based Adalimumab and Ustekinumab. Galactosylation of IgA *in planta* could reveal if the GlcNAc residue is not added or removed. The presence of terminal galactose would prevent removal of GlcNAc's. Humanising the *N*-glycans on IgA would be a necessary step in any case for future application of IgA as a biopharmaceutical.

Monoclonal IgG antibodies are expressed in several other expression platforms, such as yeast, insect cells and mammalian cells; however, production of IgA-based antibodies has also gained less attention in these platforms. In yeast for instance, only IgG-based antibodies have been expressed and were shown to carry high mannose-type *N*-glycans, which is typical for yeast (Cerutti and Golay, 2012). Insect cells also add high mannose-type *N*-glycans to IgG or paucimannosidic type *N*-glycans carrying core α1,3-fucose and/or α1,6-fucose (Cerutti and Golay, 2012; Palmberger *et al.*, 2011). Only one IgA-based antibody has been expressed in insect cells, and this antibody carried high mannose-type *N*-glycans (Carayannopoulos *et al.*, 1994). Our Infliximab also carried high mannose-type *N*-glycans, and like the insect cell-produced IgA, it is a chimeric antibody with mouse variable regions on a human backbone. In both yeast and insect cells, attempts to humanise *N*-glycosylation of IgG have been successful (Hamilton and Gerngross, 2007; Palmberger *et al.*, 2011), however, have never been evaluated for IgA. Finally, expression of IgG and IgA in different types of mammalian cells (CHO and Sp2/0) has revealed differences in *N*-glycan composition, but main differences were found in the amount and type of sialylation or galactosylation (Yoo *et al.*, 2010). As galactosylation would prevent the removal of GlcNAc's, we can only conclude that GlcNAc is efficiently added in these mammalian expression platforms. On the other hand, core α1,6-fucosylation of CHO cell-produced IgA1 was less efficient compared to IgG, but was still comparable to that of serum IgA1 (Yoo *et al.*, 2010). Due to large differences in *N*-glycosylation pathways of these different expression hosts and the limited experience with *N*-glycan analysis of IgA expressed in insect and mammalian cells, it is difficult to conclude whether or not the differences in *N*-glycosylation between plant-expressed IgG and IgA are plant-specific.

In conclusion, we have demonstrated that plants can be used equally well for the production of IgA as IgG in terms of yield and functionality. However, the *N*-glycan an antibody receives upon expression in *N. benthamiana* is determined by the isotype. Whether or not the *N*-glycans on plant-produced human IgA can be humanized is a next step that will also yield insight in the protein intrinsic properties that influence *N*-glycosylation.

Experimental procedures

Construct design

All genes required for expression of the three different antibodies (Infliximab (I), Adalimumab (A) and Ustekinumab (U) on a human IgG1κ or IgA1κ backbone) were synthetically made by GeneArt (Bleiswijk, the Netherlands). The constant domains of human immunoglobulin alpha-1 (ACC82528.1), gamma-1 (AJ294730.1) and kappa (AGH70219.1) chains were ordered in their native sequence. All variable regions and the signal peptide of the *Arabidopsis thaliana* chitinase gene (AAM10081.1) were recoded from the amino acid sequence using codons preferred by in-house codon optimization. These gene fragments were flanked by the following restriction sites at the 5′ and 3′-end for subsequent cloning steps: NcoI-EagI, EagI-NheI, NheI-KpnI, EagI-BsiWI and BsiWI-KpnI for the signal peptide, heavy chain variable regions, heavy chain constant domains, light chain variable regions and the light chain constant domain, respectively. None of the restriction sites introduced additional amino acids except NcoI, which introduced an alanine after the first methionine. Fragments were assembled using standard cloning procedures and ligated into the shuttle vector pRAPa, a pRAP (or pUCAP35S) (van Engelen *et al.*, 1994) derivative modified to include an AsiSI restriction site by introduction of the self-annealed oligo 5′-AGCTGGCGATCGCC-3′ into a HindIII linearized pRAP. The kappa chain expression cassette was digested from pRAPa with AscI and PacI and ligated into the expression vector pHYG (Westerhof *et al.*, 2012). Subsequently, the heavy chain cassettes were combined with the kappa chain expression vector using the restriction sites AscI and AsiSI, of which the latter creates the same overhang as PacI. Vectors were transformed to *Agrobacterium tumefaciens* strain MOG101 for plant expression.

Agrobacterium tumefaciens transient transformation assay

Agrobacterium tumefaciens clones were cultured overnight (o/n) at 28 °C in LB medium (10 g/L pepton140, 5 g/L yeast extract, 10 g/L NaCl with pH7.0) containing 50 μg/mL kanamycin and 20 μg/mL rifampicin. The optical density (OD) was measured at 600 nm and used to inoculate 50 mL of LB medium containing 200 μM acetosyringone and 50 μg/mL kanamycin with × μL of culture using the following formula: $x = 80\,000/(1028 \times \mathrm{OD})$. OD was measured again after 16 h, and the bacterial cultures were centrifuged for 15 min at 2800 *g*. The bacteria were resuspended in MMA infiltration medium (20 g/L sucrose, 5 g/L MS salts, 1.95 g/L MES, pH5.6) containing 200 μM acetosyringone till an OD of one was reached. All constructs were

co-expressed with the *Tomato bushy stunt virus* (TBSV) silencing inhibitor p19 by mixing *Agrobacterium* cultures 1 : 1. After 1–2 h incubation at room temperature, the two youngest fully expanded leaves of 5–6-week-old *N. benthamiana* plants were infiltrated at the abaxial side using a 1-mL syringe. Infiltrated plants were maintained in a controlled greenhouse compartment (UNIFARM, Wageningen), and infiltrated leaves were harvested at selected time points.

Apoplast soluble protein extraction

Leaves were vacuum-infiltrated with ice-cold extraction buffer (50 mM phosphate-buffered saline (PBS) pH = 7.4, 100 mM NaCl, 10 mM ethylenediaminetetraacetic acid (EDTA), 0.1% v/v Tween-20) for 10 min. Leaves were dried from the outside and placed in a 10-mL syringe hanging in a blue cap and centrifuged at 2000 ***g*** for 15 min at 4 °C. The volume of apoplast fluid was determined and directly used in an ELISA and BCA protein assay.

Total soluble protein extraction

Leaves were snap-frozen, homogenized in liquid nitrogen (after apoplast extraction or immediately upon harvesting) and stored at −80 °C until use. Homogenized plant material was ground in ice-cold extraction buffer (50 mM phosphate-buffered saline (PBS) pH = 7.4, 100 mM NaCl, 10 mM ethylenediaminetetraacetic acid (EDTA), 0.1% v/v Tween-20, 2% w/v immobilized polyvinylpolypyrrolidone (PVPP)) using 2 mL/g fresh weight. Crude extract was clarified by centrifugation at 16 000 ***g*** for 5 min at 4 °C, and supernatant was directly used in an ELISA and BCA protein assay.

IgA and IgG quantification

IgA and IgG concentrations in apoplast fluids and crude extracts were determined by sandwich ELISA using goat polyclonal anti-human kappa antibody (Sigma-Aldrich, Zwijndrecht, the Netherlands) as capture antibody. HRP-conjugated goat polyclonal antibodies (Sigma-Aldrich) directed against the constant domains of IgG and IgA were used for detection. For sample comparison, the total soluble protein (TSP) concentration was determined using the BCA protein assay (Pierce) according to supplier's protocol using bovine serum albumin (BSA) as a standard.

Protein analysis by Western blot

Fifty ng of antibody in crude extract was separated under reducing conditions by SDS-PAGE on a NuPAGE® 12% Bis-Tris gel (Life Technologies, Bleiswijk, the Netherlands) and transferred to an Invitrolon™ PVDF membrane (Life Technologies) by a wet blotting procedure. Recombinant IgG1κ (Sigma-Aldrich) or IgA1κ (InvivoGen, Toulouse, France) was used as a control. For visualization, goat polyclonal antibodies (Sigma-Aldrich) directed against human kappa or human IgA followed by incubation with a HRP-conjugated secondary antibody (Jackson ImmunoResearch, Suffolk, UK) or HRP-conjugated antibody directed against human IgG were used. SuperSignal West Femto substrate (Thermo Fisher Scientific, Etten-Leur, the Netherlands) was used to detect HRP-conjugated antibodies. Pictures were taken using a G:BOX Chemi System device (SynGene, Cambridge, UK).

Antibody purification

For purification of plant-produced antibodies, crude extracts were first desalted over G25 Sephadex columns. Plant-produced IgG was then purified using Protein G affinity matrix (Thermo Fisher Scientific), and plant-produced IgA was purified using IgA CaptureSelect affinity matrix (Life Technologies).

N-glycan analysis

IgA or IgG (in apoplast fluids, crude extracts or purified) was deglycosylated with PNGase F or Endo H (both from Bioké, Leiden, the Netherlands) to screen for the presence of plant-specific α1,3-fucosylated or oligomannose-type *N*-glycans, respectively. A Western blot using a rabbit polyclonal antihorseradish peroxidase antibody (Jackson ImmunoResearch) was used to detect plant-specific α1,3-fucose and β1,2-xylose, followed by a HRP-conjugated donkey anti-rabbit IgG (Jackson ImmunResearch).

For analysis of *N*-glycan composition, glycopeptides were prepared from 10 μg of antibody by in-gel trypsin digestion using the Trypsin Profile IGD kit (Sigma-Aldrich). Tryptic glycopeptides were purified over ZipTip$_{C18}$ (Merck, Amsterdam, the Netherlands), eluted with 18% v/v acetonitrile and analysed by MALDI-TOF-MS. For IgA *N*-glycan analysis proteolytic digestion with trypsin (Sigma-Aldrich), pepsin or thermolysin (both from Promega, Leiden, the Netherlands) was performed on 10–100 μg IgA prior to the release of *N*-glycans with 0.5 mU PNGase A (Roche, Woerden, the Netherlands). Released *N*-glycans were purified by C18 Baker-bond™ SPE cartridges (VWR, Amsterdam, the Netherlands) and subsequent Extract Clean™ Carbo SPE columns (Grace, Breda, the Netherlands). *N*-glycans were labelled with anthranilic acid (AA) (Sigma-Aldrich), desalted over Biogel P10 (BioRad, Veenendaal, The Netherlands) and analysed by MALDI-TOF-MS. Alternatively, *N*-glycans were released from 20 μg IgA by PNGase F digestion (Bioké). Released *N*-glycans were purified on Extract-Clean™ Carbograph Columns (Grace), AA-labelled and purified over ZipTip$_{C18}$ (Merck) prior to MALDI-TOF-MS analysis.

TNFα neutralization assay

L929 cells (DSMZ, Braunschweig, Germany) were cultured in RPMI-1640 medium containing 4 mM L-glutamine, 25 mM HEPES and supplemented with 10% foetal calf serum, 50 U/mL, 50 μg/mL streptomycin and 50 μM β-mercaptoethanol at 37 °C with 5% CO_2. Cells were seeded in 96-well plates at a density of 5×10^4 cells/well and allowed to rest overnight. The cells were then treated with a 10-fold serial dilution of purified plant-produced antibodies from 10 to 0.01 μg/mL in combination with 1 ng/mL recombinant *E. coli*-produced human TNF-α and 1 μg/mL Actinomycin D (both from R&D Systems, Abingdon, UK). As positive controls, mammalian cell-produced infliximab and an anti-TNF-α-IgA (InvivoGen) were used. After overnight incubation, cell viability was determined using the CellTiter 96® AQueous One Solution Cell Proliferation Assay (Promega) according to the supplier's protocol.

IL-23 neutralization assay

Splenocytes were isolated from spleens of C57BL/6 mice by passing them through a 70-μm nylon cell strainer (BD Biosciences, Breda, the Netherlands). Red blood cells were lysed using the Mouse Erythrocyte Lysing Kit (R&D Systems), and obtained splenocytes were seeded in 96-well plates at a density of 5×10^5 cells/well in RPMI-1640 medium containing 4 mM L-glutamine, 25 mM HEPES and supplemented with 10% foetal calf serum, 50 U/mL penicillin, 50 μg/mL streptomycin and 50 μM β-mercaptoethanol. Splenocytes were treated with a 10-fold serial dilution of purified plant-produced antibodies from 10 to 0.001 μg/mL in combination with 1 ng/mL recombinant *E. coli*-produced human IL-23 and 10 ng/mL PMA. As positive control, mammalian cell-produced Ustekinumab was used. After 5 days, supernatants were analysed for IL-17 expression with the

mouse IL-17 Ready-Set-Go! ELISA Kit (eBioscience, Vienna, Austria) according to the supplier's protocol.

Acknowledgements

We declare no conflict of interest. We would also like to thank Tim Warbroek, Aleksandra Syta and Bob Engelen for their input in the experimental work of this paper.

References

Bain, B. and Brazil, M. (2003) Adalimumab. *Nat. Rev. Drug Discovery*, **2**, 693–694.

Bakema, J.E. and van Egmond, M. (2011) Immunoglobulin A: a next generation of therapeutic antibodies? *MAbs*, **3**, 352–361.

Bednarek, S.Y., Wilkins, T.A., Dombrowski, J.E. and Raikhel, N.V. (1990) A carboxyl-terminal propeptide is necessary for proper sorting of barley lectin to vacuoles of tobacco. *Plant Cell*, **2**, 1145–1155.

Bosch, D., Castilho, A., Loos, A., Schots, A. and Steinkellner, H. (2013) N-Glycosylation of plant-produced recombinant proteins. *Curr. Pharm. Des.* **19**, 5503–5512.

Carayannopoulos, L., Max, E.E. and Capra, J.D. (1994) Recombinant human IgA expressed in insect cells. *Proc. Natl Acad. Sci. USA*, **91**, 8348–8352.

Castilho, A., Bohorova, N., Grass, J., Bohorov, O., Zeitlin, L., Whaley, K., Altmann, F. and Steinkellner, H. (2011) Rapid high yield production of different glycoforms of ebola virus monoclonal antibody. *PLoS One*, **6**, e26040.

Cerutti, M. and Golay, J. (2012) Lepidopteran cells, an alternative for the production of recombinant antibodies? *MAbs*, **4**, 294–309.

Cox, K.M., Sterling, J.D., Regan, J.T., Gasdaska, J.R., Frantz, K.K., Peele, C.G., Black, A., Passmore, D., Moldovan-Loomis, C., Srinivasan, M., Cuison, S., Cardarelli, P.M. and Dickey, L.F. (2006) Glycan optimization of a human monoclonal antibody in the aquatic plant Lemna minor. *Nat. Biotechnol.* **24**, 1591–1597.

De Muynck, B., Navarre, C. and Boutry, M. (2010) Production of antibodies in plants: status after twenty years. *Plant Biotechnol. J.* **8**, 529–563.

Ebert, E.C. (2009) Infliximab and the TNF-alpha system. *Am J Physiol Gastrointest Liver Physiol.* **296**, G612–G620.

van Engelen, F.A., Schouten, A., Molthoff, J.W., Roosien, J., Salinas, J., Dirkse, W.G., Schots, A., Bakker, J., Gommers, F.J., Jongsma, M.A., Bosch, D. and Stiekema, W.J. (1994) Coordinate expression of antibody subunit genes yields high levels of functional antibodies in roots of transgenic tobacco. *Plant Mol. Biol.* **26**, 1701–1710.

Field, M.C., Amatayakul-Chantler, S., Rademacher, T.W., Rudd, P.M. and Dwek, R.A. (1994) Structural analysis of the N-glycans from human immunoglobulin A1: comparison of normal human serum immunoglobulin A1 with that isolated from patients with rheumatoid arthritis. *Biochem. J.* **299** (Pt 1), 261–275.

Fitchettelaine, A.C., Gomord, V., Chekkafi, A. and Faye, L. (1994) Distribution of xylosylation and fucosylation in the plant Golgi-apparatus. *Plant J.* **5**, 673–682.

Frigerio, L., Vine, N.D., Pedrazzini, E., Hein, M.B., Wang, F., Ma, J.K.C. and Vitale, A. (2000) Assembly, secretion, and vacuolar delivery of a hybrid immunoglobulin in plants. *Plant Physiol.* **123**, 1483–1493.

Gandhi, M., Alwawi, E. and Gordon, K.B. (2010) Anti-p40 antibodies Ustekinumab and Briakinumab: blockade of interleukin-12 and interleukin-23 in the treatment of psoriasis. *Semin. Cutan. Med. Surg.* **29**, 48–52.

Hadlington, J.L., Santoro, A., Nuttall, J., Denecke, J., Ma, J.K.C., Vitale, A. and Frigerio, L. (2003) The C-terminal extension of a hybrid immunoglobulin A/G heavy chain is responsible for its Golgi-mediated sorting to the vacuole. *Mol. Biol. Cell*, **14**, 2592–2602.

Hamilton, S.R. and Gerngross, T.U. (2007) Glycosylation engineering in yeast: the advent of fully humanized yeast. *Curr. Opin. Biotechnol.* **18**, 387–392.

Herr, A.B., Ballister, E.R. and Bjorkman, P.J. (2003) Insights into IgA-mediated immune responses from the crystal structures of human FcalphaRI and its complex with IgA1-Fc. *Nature*, **423**, 614–620.

Hiatt, A. and Pauly, M. (2006) Monoclonal antibodies from plants: a new speed record. *Proc. Natl Acad. Sci. USA*, **103**, 14645–14646.

Huls, G., Heijnen, I.A., Cuomo, E., van der Linden, J., Boel, E., van de Winkel, J.G. and Logtenberg, T. (1999) Antitumor immune effector mechanisms recruited by phage display-derived fully human IgG1 and IgA1 monoclonal antibodies. *Cancer Res.* **59**, 5778–5784.

Juarez, P., Presa, S., Espı, J., Pineda, B., Anton, M.T., Moreno, V., Buesa, J., Granell, A. and Orzaez, D. (2012) Neutralizing antibodies against rotavirus produced in transgenically labelled purple tomatoes. *Plant Biotechnol. J.* **10**, 341–352.

Kajiura, H., Okamoto, T., Misaki, R., Matsuura, Y. and Fujiyama, K. (2012) Arabidopsis beta 1,2-xylosyltransferase: substrate specificity and participation in the plant-specific N-glycosylation pathway. *J. Biosci. Bioeng.* **113**, 48–54.

Karnoup, A.S., Turkelson, V. and Anderson, W.H. (2005) O-linked glycosylation in maize-expressed human IgA1. *Glycobiology*, **15**, 965–981.

Koide, Y., Matsuoka, K., Ohto, M. and Nakamura, K. (1999) The N-terminal propeptide and the C terminus of the precursor to 20-kilo-dalton potato tuber protein can function as different types of vacuolar sorting signals. *Plant Cell Physiol.* **40**, 1152–1159.

Liebminger, E., Veit, C., Pabst, M., Batoux, M., Zipfel, C., Altmann, F., Mach, L. and Strasser, R. (2011) beta-N-Acetylhexosaminidases HEXO1 and HEXO3 are responsible for the formation of Paucimannosidic N-Glycans in *Arabidopsis thaliana*. *J. Biol. Chem.* **286**, 10793–10802.

Ma, J.K.-C., Lehner, T., Stabila, P., Fux, C.I. and Hiatt, A. (1994) Assembly of monoclonal antibodies with IgG1 and IgA heavy chain domains in transgenic tobacco plants. *Eur. J. Immunol.* **24**, 131–138.

Mattu, T.S., Pleass, R.J., Willis, A.C., Kilian, M., Wormald, M.R., Lellouch, A.C., Rudd, P.M., Woof, J.M. and Dwek, R.A. (1998) The glycosylation and structure of human serum IgA1, Fab, and Fc regions and the role of N-glycosylation on Fc alpha receptor interactions. *J. Biol. Chem.* **273**, 2260–2272.

Nakanishi, K., Narimatsu, S., Ichikawa, S., Tobisawa, Y., Kurohane, K., Niwa, Y., Kobayashi, H. and Imai, Y. (2013) Production of hybrid-IgG/IgA plantibodies with neutralizing activity against Shiga toxin 1. *PLoS One*, **8**, e80712.

Neuhaus, J.M. and Rogers, J.C. (1998) Sorting of proteins to vacuoles in plant cells. *Plant Mol. Biol.* **38**, 127–144.

Neuhaus, J.M., Sticher, L., Meins, F. Jr and Boller, T. (1991) A short C-terminal sequence is necessary and sufficient for the targeting of chitinases to the plant vacuole. *Proc. Natl Acad. Sci. USA*, **88**, 10362–10366.

Nicholson, L., Gonzalez-Melendi, P., van Dolleweerd, C., Tuck, H., Perrin, Y., Ma, J.K.C., Fischer, R., Christou, P. and Stoger, E. (2005) A recombinant multimeric immunoglobulin expressed in rice shows assembly-dependent subcellular localization in endosperm cells. *Plant Biotechnol. J.* **3**, 115–127.

Palmberger, D., Rendic, D., Tauber, P., Krammer, F., Wilson, I.B. and Grabherr, R. (2011) Insect cells for antibody production: evaluation of an efficient alternative. *J. Biotechnol.* **153**, 160–166.

Park, M., Kim, S.J., Vitale, A. and Hwang, I. (2004) Identification of the protein storage vacuole and protein targeting to the vacuole in leaf cells of three plant species. *Plant Physiol.* **134**, 625–639.

Petrescu, A.J., Milac, A.L., Petrescu, S.M., Dwek, R.A. and Wormald, M.R. (2004) Statistical analysis of the protein environment of N-glycosylation sites: implications for occupancy, structure, and folding. *Glycobiology*, **14**, 103–114.

Pucic, M., Knezevic, A., Vidic, J., Adamczyk, B., Novokmet, M., Polasek, O., Gornik, O., Supraha-Goreta, S., Wormald, M.R., Redzic, I., Campbell, H., Wright, A., Hastie, N.D., Wilson, J.F., Rudan, I., Wuhrer, M., Rudd, P.M., Josic, D. and Lauc, G. (2011) High throughput isolation and glycosylation analysis of IgG-variability and heritability of the IgG glycome in three isolated human populations. *Mol. Cell. Proteomics*, **10**, M111.010090.

Rayon, C., Lerouge, P. and Faye, L. (1998) The protein N-glycosylation in plants. *J. Exp. Bot.* **49**, 1463–1472.

Schillberg, S., Fischer, R. and Emans, N. (2003) Molecular farming of recombinant antibodies in plants. *Cell. Mol. Life Sci.* **60**, 433–445.

Shen, C., Assche, G.V., Colpaert, S., Maerten, P., Geboes, K., Rutgeerts, P. and Ceuppens, J.L. (2005) Adalimumab induces apoptosis of human monocytes: a comparative study with infliximab and etanercept. *Aliment. Pharmacol. Ther.* **21**, 251–258.

Snoeck, V., Peters, I.R. and Cox, E. (2006) The IgA system: a comparison of structure and function in different species. *Vet. Res.* **37**, 455–467.

Stoop, J.W., Zegers, B.J., Sander, P.C. and Ballieux, R.E. (1969) Serum immunoglobulin levels in healthy children and adults. *Clin. Exp. Immunol.* **4**, 101–112.

Strasser, R., Singh, J., Bondili, J.S., Schoberer, J., Svoboda, B., Liebminger, E., Glossl, J., Altmann, F., Steinkellner, H. and Mach, L. (2007) Enzymatic properties and subcellular localization of Arabidopsis beta-N-acetylhexosaminidases. *Plant Physiol.* **145**, 5–16.

Strasser, R., Castilho, A., Stadlmann, J., Kunert, R., Quendler, H., Gattinger, P., Jez, J., Rademacher, T., Altmann, F., Mach, L. and Steinkellner, H. (2009) Improved virus neutralization by plant-produced anti-HIV antibodies with a homogeneous beta1,4-galactosylated N-glycan profile. *J. Biol. Chem.* **284**, 20479–20485.

Van den Brande, J.M., Braat, H., van den Brink, G.R., Versteeg, H.H., Bauer, C.A., Hoedemaeker, I., van Montfrans, C., Hommes, D.W., Peppelenbosch, M.P. and van Deventer, S.J. (2003) Infliximab but not etanercept induces apoptosis in lamina propria T-lymphocytes from patients with Crohn's disease. *Gastroenterology*, **124**, 1774–1785.

Van der Steen, L., Tuk, C.W., Bakema, J.E., Kooij, G., Reijerkerk, A., Vidarsson, G., Bouma, G., Kraal, G., de Vries, H.E., Beelen, R.H. and van Egmond, M. (2009) Immunoglobulin A: Fc(alpha)RI interactions induce neutrophil migration through release of leukotriene B4. *Gastroenterology*, **137**, 2018–2029, e1–3.

Vitale, A. and Raikhel, N.V. (1999) What do proteins need to reach different vacuoles? *Trends Plant Sci.* **4**, 149–155.

Westerhof, L.B., Wilbers, R.H.P., Roosien, J., van de Velde, J., Goverse, A., Bakker, J. and Schots, A. (2012) 3D domain swapping causes extensive multimerisation of human interleukin-10 when expressed in planta. *PLoS One*, **7**, e46460.

Wieland, W.H., Lammers, A., Schots, A. and Orzaez, D.V. (2006) Plant expression of chicken secretory antibodies derived from combinatorial libraries. *J. Biotechnol.* **122**, 382–391.

Yoo, E.M., Yu, L.J., Wims, L.A., Goldberg, D. and Morrison, S.L. (2010) Differences in N-glycan structures found on recombinant IgA1 and IgA2 produced in murine myeloma and CHO cell lines. *MAbs*, **2**, 320–334.

Supporting information

Additional Supporting information may be found in the online version of this article:

Figure S1 *N*-glycan types carried by the plant-produced IgG1κ variants of Infliximab (I), Adalimumab (A) and Ustekinumab (U) as determined using MALDI-TOF-MS.

Figure S2 *N*-glycan types carried by the plant-produced IgA1κ variants of Infliximab (I), Adalimumab (A) and Ustekinumab (U) as determined using MALDI-TOF-MS.